IJST, Transactions of Electrical Engineering, Vol. 35, No. E1, pp 63-74
Printed in The Islamic Republic of Iran, 2011
© Shiraz University

IMPLEMENTATION OF SENSORLESS SPEED CONTROL FOR TWO-PHASE INDUCTION MOTOR DRIVE USING ISFOC STRATEGY*

H. BEN AZZA[1**] M. JEMLI[1], M. BOUSSAK[2] AND M. GOSSA[1]

[1] Unité de recherche en commande, surveillance et sûreté de fonctionnement des systèmes (C3S)
Equipe Développement des Systèmes Electrotechniques (DES)
Ecole Supérieure des Sciences et Techniques de Tunis (ESSTT)
5 Avenue Taha Hussein –BP 56, Bab Mnara 1008 Tunis – Tunisie
Email: benazzahechmi@voila.fr
[2] Laboratoire des Sciences de l'Information et des Systèmes (LSIS) – UMR CNRS 6168
Centrale Marseille Recherche et Technologies (CMRT)
Ecole Centrale Marseille (ECM) – Technopôle Château Gombert –13451 – Marseille Cedex 20 – France

Abstract– This paper presents a new technique based on model reference adaptive system (MRAS) observer for sensorless speed control of Two-Phase Induction Motor (TPIM). The MRAS identification is performed by means of comparison of stator fluxes obtained from both stator and rotor equations with stator voltage and current measurements. Simulation and experimental results for a 1.1 kW TPIM set-up are presented and analysed using a dSpace system with a DS1104 controller board based on digital signal processor (DSP) TMS320F240. Simulation and experimental results at nominal, low and zero speeds confirm the effectiveness of the proposed sensorless speed controlled TPIM drive.

Keywords– Two-phase induction motor (TPIM), indirect stator-field-oriented control (ISFOC), model reference adaptive system (MRAS)

1. INTRODUCTION

Two-Phase Induction Motor (TPIM) is widely used in several industrial and domestic applications. In those applications the motor runs at constant frequency and is fed directly from the ac grid without any type of control strategy. The TPIM is found in air conditioners, washers, dryers, industrial machinery, fans, compressors, tools, blowers, vacuum cleaners, household appliances and many other applications. The reduction in the cost of the power electronic circuitry provides economically justifiable applications for adjustable speed Two-Phase Induction Motor Drives (TPIMD). In recent years, several methods that use inverters for the variable speed control of TPIM have been proposed [1]-[15]. An alternative approach is to use a 6 switch three phase Voltage-Source Inverter (VSI) bridge, connecting the two windings of the motor as an unbalanced load between the phases, as shown in Fig. 3. This is a more cost effective solution [1], [2], [9], [11], [16]. Recently, Stator Field Oriented Control (SFOC) of TPIMD has been gaining wide attention in literature [1]-[3]. In vector control, the flux linkage magnitude and the electromagnetic torque are controlled independently [14]-[15]. The SFOC represents a better solution to satisfy the industrial requirements. The field orientation is relatively straightforward in all operating conditions if the rotor speed is accurately known, which traditionally necessitates a sensor on the shaft of the motor. However, there are several reasons for preferring a system without the sensor. The cost of the speed sensor, at least for machines with ratings less than 10 kW, is in the same range as the cost of the motor itself. The

*Received by the editors July 17, 2010; Accepted June 13, 2011.
**Corresponding author

mounting of the sensor to the motor is also an obstacle in many applications. A Sensorless system where the speed is estimated instead of measured would essentially reduce the cost and complexity of the drive system. In the existing literature, some approaches have been suggested for speed Sensorless single-phase induction motor in [2], [3], [15], [17], [18], [19] and [20]. In papers [2] and [3], the authors proposed a method of rotor speed estimation based only on the measurement of the main and auxiliary windings stator currents and that of a reference q-axis current generated by the control algorithm. In [20], the authors suggested to estimate the motor speed using rotor voltage vector which is defined in complex domain. In this paper, for the first time, a speed estimation method is introduced for TPIMs based on the Model Reference Adaptive System (MRAS) to overcome the problems of system complexity and cost. The Sensorless speed control strategy using MRAS techniques is based on the comparison between the outputs of two estimators when motor currents and voltages must still be measured [21], [22]. In this paper we focus on a real implementation using DS1104 controller board of Indirect Stator Field Oriented Control (ISFOC) of a TPIM supplied by Proportional plus Integral (PI) current controlled inverter. Our contribution is real time implementation of a Sensorless speed control using the MRAS approach. Simulation and experimental results are presented to demonstrate the main characteristics of the proposed drive system. The Sensorless speed control algorithm is employed in this work and is implemented at rated, low, and zero speed operations

2. TWO-PHASE INDUCTION MOTOR MODEL

The set of equations that defines the dynamic model for TPIM in a stationary reference frame is given by:

$$v_{s\alpha} = R_{sd} i_{s\alpha} + \frac{d\phi_{s\alpha}}{dt} \tag{1}$$

$$v_{s\beta} = R_{sq} i_{s\beta} + \frac{d\phi_{s\beta}}{dt} \tag{2}$$

$$0 = R_r i_{r\alpha} + \frac{d\phi_{r\alpha}}{dt} + \omega\phi_{r\beta} \tag{3}$$

$$0 = R_r i_{r\beta} + \frac{d\phi_{r\beta}}{dt} - \omega\phi_{r\alpha} \tag{4}$$

$$\phi_{s\alpha} = L_{sd} i_{s\alpha} + M_{srd} i_{r\alpha} \tag{5}$$

$$\phi_{s\beta} = L_{sq} i_{s\beta} + M_{srq} i_{r\beta} \tag{6}$$

$$\phi_{r\alpha} = L_r i_{r\alpha} + M_{srd} i_{s\alpha} \tag{7}$$

$$\phi_{r\beta} = L_r i_{r\beta} + M_{srq} i_{s\beta} \tag{8}$$

$$T_e = n_p (M_{srq} i_{s\beta} i_{r\alpha} - M_{srd} i_{s\alpha} i_{r\beta}) \tag{9}$$

It is seen that Eqs. (1) to (8) present the model of an asymmetrical TPIM due to the unequal resistances and inductances of the main and auxiliary windings. This asymmetry causes an oscillating term in the electromagnetic torque [1]. In order to simplify the mathematical model of a TPIM it is necessary, as a first step, to introduce a transformation matrix $T = \begin{bmatrix} 1 & 0 \\ 0 & k \end{bmatrix}$ for the stator variables. Using this matrix we can write:

$$i_{s\alpha\beta} = T i_{s\alpha\beta 1} \tag{10}$$

$$v_{s\alpha\beta} = T^{-1} v_{s\alpha\beta 1} \tag{11}$$

$$\phi_{s\alpha\beta} = T^{-1} \phi_{s\alpha\beta 1} \tag{12}$$

where: $k = \dfrac{M_{srd}}{M_{srq}}$

Using Eqs. (1) to (12), the new mathematical model of the TPIM in a stationary reference frame can be described by the following equations:

$$v_{s\alpha 1} = R_{sd} i_{s\alpha 1} + \frac{d\phi_{s\alpha 1}}{dt} \tag{13}$$

$$v_{s\beta 1} = R_{sd}\ i_{s\beta 1} + \frac{d\phi_{s\beta 1}}{dt} + (k^2 R_{sq} - R_{sd}) i_{s\beta 1} \tag{14}$$

$$0 = R_r i_{r\alpha} + \frac{d\phi_{r\alpha}}{dt} + \omega \phi_{r\beta} \tag{15}$$

$$0 = R_r i_{r\beta} + \frac{d\phi_{r\beta}}{dt} - \omega \phi_{r\alpha} \tag{16}$$

$$\phi_{s\alpha 1} = L_{sd} i_{s\alpha 1} + M_{srd} i_{r\alpha} \tag{17}$$

$$\phi_{s\beta 1} = L_{sd} i_{s\beta 1} + M_{srd} i_{r\beta} + (k^2 L_{sq} - L_{sd}) i_{s\beta 1} \tag{18}$$

$$\phi_{r\alpha} = L_r i_{r\alpha} + M_{srd} i_{s\alpha 1} \tag{19}$$

$$\phi_{r\beta} = L_r i_{r\beta} + M_{srd} i_{s\beta 1} \tag{20}$$

$$T_e = n_p M_{srd} (i_{s\beta 1} i_{r\alpha} - i_{s\varepsilon 1} i_{r\beta}) \tag{21}$$

3. INDIRECT STATOR FIELD ORIENTED CONTROL (ISFOC)

Using Eqs. (17), (18) and (21), electromagnetic torque as a function of stator fluxes and stator currents can be written as:

$$T_e = n_p (\phi_{s\alpha 1} i_{s\beta 1} - \phi_{s\beta 1} i_{s\alpha 1} + \Delta T) \tag{22}$$

where: $\Delta T = (k^2 L_{sq} - L_{sd}) i_{s\beta 1} i_{s\alpha 1}$

In the same way, using Eqs. (15-20), we can determine the dynamic model that relates the stator flux to the stator currents:

$$\frac{d\phi_{s\alpha 1}}{dt} + \frac{1}{\tau}\phi_{s\alpha 1} + \omega \phi_{s\beta 1} = \frac{L_{sd}}{\tau_r} i_{s\alpha 1} + \sigma_d L_{sd} \frac{di_{s\alpha 1}}{dt} + \omega k^2 \sigma_q L_{sq} i_{s\beta 1} \tag{23}$$

$$\frac{d\phi_{s\beta 1}}{dt} + \frac{1}{\tau_r}\phi_{s\beta 1} - \omega \phi_{s\alpha 1} = k^2 \frac{L_{sq}}{\tau_r} i_{s\beta 1} + k^2 \sigma_q L_{sq} \frac{di_{s\beta 1}}{dt} - \omega \sigma_d L_{sd} i_{s\alpha 1} \tag{24}$$

in which: $\sigma_d = 1 - \dfrac{M_{srd}^2}{L_{sd} L_r}$, $\sigma_q = 1 - \dfrac{M_{srq}^2}{L_{sq} L_r}$, $\tau_{sd} = \dfrac{L_{sd}}{R_{sd}}$, $\tau_{sq} = \dfrac{L_{sq}}{R_{sq}}$ and $\tau_r = \dfrac{L_r}{R_r}$.

The vector model for the stator-flux control written for an arbitrary frame (denoted by the superscript *a*) using Eqs. (23) and (24) are given by:

$$\frac{d\phi_{sl}^{a}}{dt}+\frac{1}{\tau_r}\phi_{sl}^{a}+j(\omega_a-\omega)\phi_{sl}^{a}=\frac{L_{sd}}{\tau_r}i_{sl}^{a}+\sigma_d L_{sd}\frac{di_{sl}^{a}}{dt}+j(\omega_a-\omega)\sigma_d L_{sd}i_{sl}^{a}+\varsigma_s^{a} \tag{25}$$

where: $\phi_{sl}^{a}=\phi_{s\alpha 1}^{a}+j\phi_{s\beta 1}^{a}=(\phi_{s\alpha 1}+j\phi_{s\beta 1})e^{-j\delta_a}$

$$i_{sl}^{a}=i_{s\alpha 1}^{a}+ji_{s\beta 1}^{a}=(i_{s\alpha 1}+ji_{s\beta 1})e^{-j\delta_a}$$

$$\varsigma_s^{a}=\left(k^2L_{sq}-L_{sd}\right)\left[\left(\omega+j\frac{1}{\tau_r}\right)i_{s\beta 1}+j\frac{di_{s\beta 1}}{dt}\right]e^{-j\delta_a}$$

We choose a reference frame linked to the stator flux, so that the d axis coincides with the desired direction of the stator flux ($\phi_{sd1}=\phi_{sl}$ and $\phi_{sq1}=0$). Therefore, in this synchronous rotating reference, the expression (23) can be decomposed into two equations.

$$\frac{d\phi_{sl}}{dt}+\frac{1}{\tau_r}\phi_{sl}=\frac{L_{sd}}{\tau_r}i_{sd1}+\sigma_d L_{sd}\frac{di_{sd1}}{dt}-\omega_{sl}\sigma_d L_{sd}i_{sq1}+\varsigma_d \tag{26}$$

$$\omega_{sl}\phi_{sl}=\frac{L_{sd}}{\tau_r}i_{sq1}+\sigma_d L_{sd}\frac{di_{sq1}}{dt}+\omega_{sl}\sigma_d L_{sd}i_{sd1}+\varsigma_q \tag{27}$$

where:

$\omega_{sl}=\omega_s-\omega$: slip angular frequency;
ω_s : synchronous angular frequency;
ϕ_{sl} : stator-flux magnitude.

It is noteworthy that the model of the stator flux (Eqs. (26) and (27)) and the expression of the torque (Eq. (22)) present additional terms (ς_d, ς_q and ΔT) that represent the asymmetry of the machine. Note that these terms depend on $(k^2L_{sq}-L_{sd})$. Considering that ς_d as well as ς_q and ΔT are negligible, the model becomes symmetric and the conventional stator-field-oriented control strategy can be used [1]. If we consider that the stator flux and the electromagnetic torque are taken as control references, the following model is obtained (from Eqs. (26) and (27)):

$$i_{sd1}^{*}=\frac{(\tau_r p+1)\phi_{sl}^{*}+\tau_r\sigma_d L_{sd}i_{sq1}^{*}\omega_{sl}^{*}}{L_{sd}(1+\sigma_d\tau_r p)} \tag{28}$$

$$i_{sq1}^{*}=\frac{\left(\phi_{sl}^{*}-\sigma_d L_{sd}i_{sd1}^{*}\right)\tau_r\omega_{sl}^{*}}{L_{sd}(1+\sigma_d\tau_r p)} \tag{29}$$

4. MRAS ALGORITHM FOR SPEED ESTIMATION

a) Stator flux based MRAS speed estimation

Stator-flux based MRAS speed estimation is based on the fact that there are two ways to estimate the stator fluxes from the basic equations of the TPIM in the stationary reference frame.

- *From the stator equations:*

$$\begin{cases} \phi_{s\alpha}^{s} = \int_0^t (v_{s\alpha} - R_{sd} i_{s\alpha})dt \\ \phi_{s\beta}^{s} = \int_0^t (v_{s\beta} - R_{sq} i_{s\beta})dt \end{cases} \tag{30}$$

- *From the rotor equations:*

$$\begin{cases} \phi_{s\alpha}^{r} = \dfrac{\tau_r}{(1+\tau_r p)}\left[k\sigma_q L_{sq}\omega i_{s\beta} + \dfrac{L_{sd}}{\tau_r}(1+\sigma_d\tau_r p) i_{sd} - k\omega\phi_{s\beta}\right] \\ \phi_{sq}^{r} = \dfrac{\tau_r}{(1+\tau_r p)}\left[-\dfrac{1}{k}\sigma_d L_{sd}\omega i_{s\alpha} + \dfrac{L_{sq}}{\tau_r}(1+\sigma_q\tau_r p) i_{s\beta} + \dfrac{1}{k}\omega\phi_{s\alpha}\right] \end{cases} \tag{31}$$

Notice that the stator equations are independent of the rotor speed and are used as the reference model. The rotor equations are dependent on the rotor speed and thus can be used as the adjustable model. The system (31) leading to the so-called rotor observation is developed as:

$$p\begin{bmatrix} \phi_{s\alpha}^{r} \\ \phi_{s\beta}^{r} \end{bmatrix} = \begin{bmatrix} -\dfrac{1}{\tau_r} & -k\omega \\ \dfrac{1}{k}\omega & -\dfrac{1}{\tau_r} \end{bmatrix}\begin{bmatrix} \phi_{s\alpha}^{r} \\ \phi_{s\beta}^{r} \end{bmatrix} + \begin{bmatrix} \dfrac{L_{sd}}{\tau_r}(1+\sigma_d\tau_r p) & k\sigma_q L_{sq}\omega \\ -\dfrac{1}{k}\sigma_d L_{sd}\omega & \dfrac{L_{sq}}{\tau_r}(1+\sigma_q\tau_r p) \end{bmatrix}\begin{bmatrix} i_{s\alpha} \\ i_{s\beta} \end{bmatrix} \tag{32}$$

In this paper we propose the application of MRAS to estimate the rotor speed of vector controlled TPIM by using the output error between the models of the stator flux observations (Fig. 1).

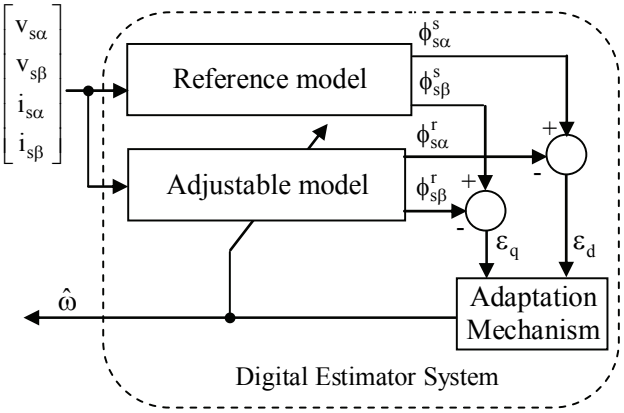


Fig. 1. Block scheme of MRAS for speed estimation

b) Adaptive estimation of the rotor speed

The main idea of the MRAS is to compare the outputs of the two models and to adjust the value of rotor speed in order to minimize the resultant error. The adjustment value is the speed generated from the error between stator fluxes observation.

The state flux error component is:

$$p\begin{bmatrix} \varepsilon_d \\ \varepsilon_q \end{bmatrix} = \begin{bmatrix} -\dfrac{1}{\tau_r} & -k\omega \\ \dfrac{1}{k}\omega & -\dfrac{1}{\tau_r} \end{bmatrix}\begin{bmatrix} \varepsilon_d \\ \varepsilon_q \end{bmatrix} + \begin{bmatrix} -k\phi_{s\beta}^{r} + k\sigma_q L_{sq} i_{s\beta} \\ \dfrac{1}{k}\phi_{s\alpha}^{r} - \dfrac{1}{k}\sigma_d L_{sd} i_{s\alpha} \end{bmatrix}(\omega - \hat{\omega}) \tag{33}$$

where: $p[\varepsilon] = [A][\varepsilon] - [W]$

$$\varepsilon_d = \phi_{s\alpha}^{s} - \phi_{s\alpha}^{r}$$

$$\varepsilon_q = \phi^s_{s\beta} - \phi^r_{s\beta}$$

$$\varepsilon = \begin{bmatrix} \varepsilon_d \\ \varepsilon_q \end{bmatrix}$$

$$A = \begin{bmatrix} -\frac{1}{\tau_r} & -k\omega \\ \frac{1}{k}\omega & -\frac{1}{\tau_r} \end{bmatrix}$$

$$[W] = \begin{bmatrix} k\phi^r_{s\beta} - k\sigma_q L_{sq} i_{s\beta} \\ -\frac{1}{k}\phi^r_{s\alpha} + \frac{1}{k}\sigma_d L_{sd} i_{s\alpha} \end{bmatrix} (\omega - \hat{\omega})$$

Where: $[W]$ is the feedback block.

In Fig. 2, the term of $[W]$ is the input and $[\varepsilon]$ is the output of the linear feed forward block and it can be easily shown that the linear equivalent system will be completely observable and controllable. The form state Eq. (33) describes the equivalent MRAS in a linear way as it was previously specified that $[\varepsilon]$ is the main information upon which differences existing between the adjustable model and the reference model can be based.

The asymptotic behavior of the adaptation mechanism is achieved by the simplified condition $\lim [\varepsilon(\infty)] = 0$ for any initialization.

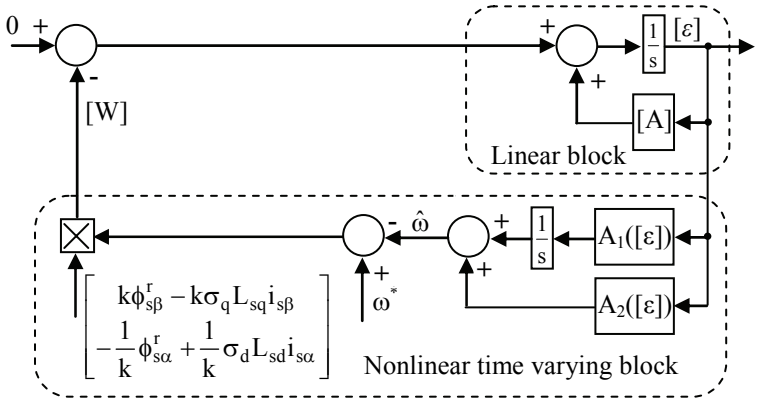


Fig. 2. Equivalent representation of nonlinear and time-varying feedback system

The feedback system will be hyper stable for any feedback block of the class satisfying the inequality:

$$\int_{t_0}^{t_1} [\varepsilon]^T [W] dt \geq -\delta_0^2 \quad \text{for all} \quad t_1 \geq t_0 \tag{34}$$

where: δ_0 is a finite positive constant.

The necessary and sufficient condition for the feedback system to be hyper stable is as follows: $H(s) = [sI - A]^{-1}$ must be a strictly positive real transfer matrix. From the previous Eq. (33) and Popov inequality, it can be easily shown that the observed speed satisfies the relationship.

$$\hat{\omega} = \frac{1}{p} A_1([\varepsilon]) + A_2([\varepsilon]) \tag{35}$$

with:
$$A_1 = K_2 \left[\left(\phi^s_{s\beta} \phi^r_{s\alpha} - \phi^s_{s\alpha} \phi^r_{s\beta} \right) - \left(i_{s\alpha} \varepsilon_q - i_{s\beta} \varepsilon_d \right) \sigma_q L_{sq} \right]$$
$$A_2 = K_1 \left[\left(\phi^s_{s\beta} \phi^r_{s\alpha} - \phi^s_{s\alpha} \phi^r_{s\beta} \right) - \left(i_{s\alpha} \varepsilon_q - i_{s\beta} \varepsilon_d \right) \sigma_d L_{sd} \right]$$

As the coefficients K_1 and K_2 of the PI regulator are involved in a non-linear system, there are no rigorous methods to compute them. Moreover, a linearization around a working point is possible, but it is preferable to find K_1 and K_2 from simulation of the complete system.

The Block diagram of speed Sensorless ISFOC for TPIM drive as illustrated in Fig. 3, where ω_{sl}^* and ϕ_{sl}^* represent the reference slip angular speed and the reference flux, respectively. The $e^{j\theta_s}$ block performs the coordinate transformation from the reference frame aligned along with the stator flux vector to the stationary reference frame.

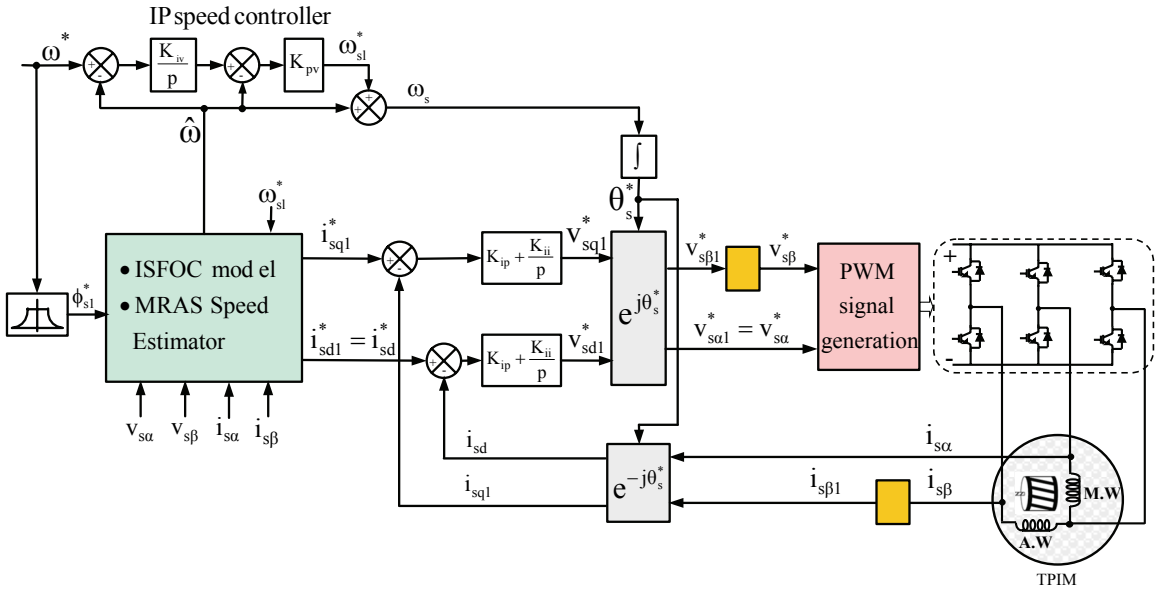


Fig. 3. Block diagram of speed Sensorless ISFOC for TPIM drive

5. EXPERIMENTAL IMPLEMENTATION

To evaluate the performance of the proposed Sensorless ISFOC speed controller, the control algorithm has been implemented using a dSpace board. The dSpace works on a Matlab/Simlink platform which is a common engineering software and easy to understand and the system is controlled by software running on a dSpace DS1104 processor board. This board contains a Motorola Power PC 603e model that operates at a speed of 250 MHz and a DSP (TMS320F240 – 20 MHz). The controller is interfaced to the real system via graphical I/O-interface blocks provided by dSpace for their DS1104 hardware. Real Time Interface (RTI) is the link between dSpace real time systems and the development software Matlab/Simulink from the Math Works. It extends Real Time Workshop (C code generation) for the automatic implementation of our Simulink. The process can be commanded and monitored via the ControlDesk software of dSpace. The scheme used for the experimental setup is shown in Fig. 4.

The TPIMD is fed by a three-leg voltage source inverter (VSI) using six Insulate Bipolar Transistors (IGBT). As shown in Fig. 4, the one end of the main and auxiliary windings of the motor are connected to one half bridge each. The other ends are tied together and connected to the third half bridge. In order to reduce the ripple current of the TPIMD, a suitable PWM was implemented for the three-leg two-phase output voltages inverter. We propose sinusoidal PWM method instead of Space Vector Pulse Wide Modulation (SVPWM). In a three-leg inverter, two legs control the main and auxiliary winding of the TPIMD voltages and one leg controls the offset voltage. In the experimental test we realise PWM signals for the three leg two-phase inverter in the following way:

- PWM duty cycle is calculated according to v_{sdref} for leg 1,
- PWM duty cycle is calculated according to v_{sqref} for leg 2,
- Duty cycle is taken constant equal to 0.5 to provide a zero reference voltage for leg 3.

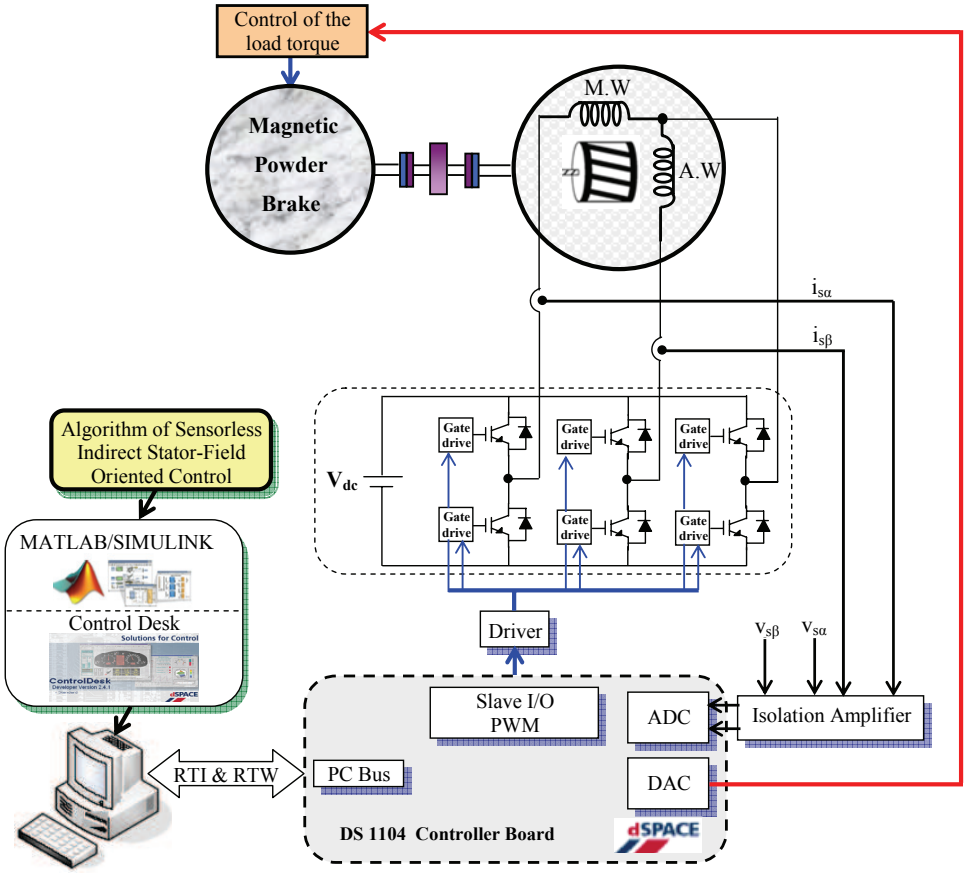
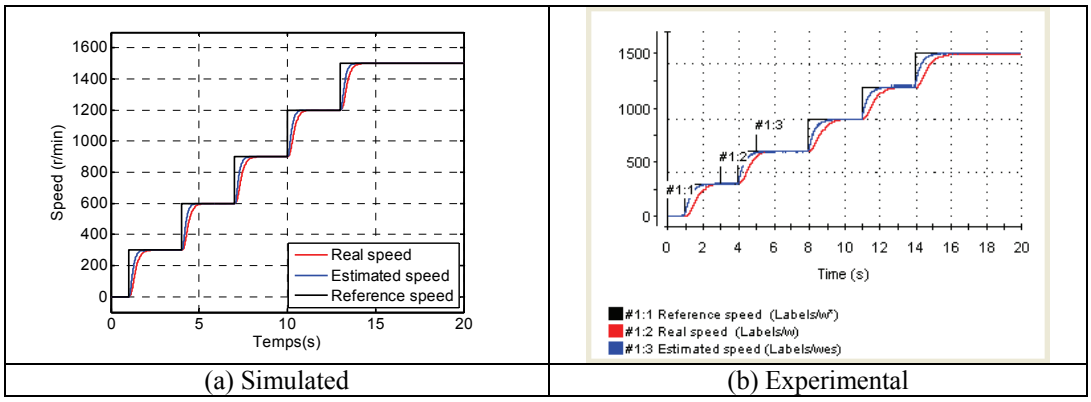


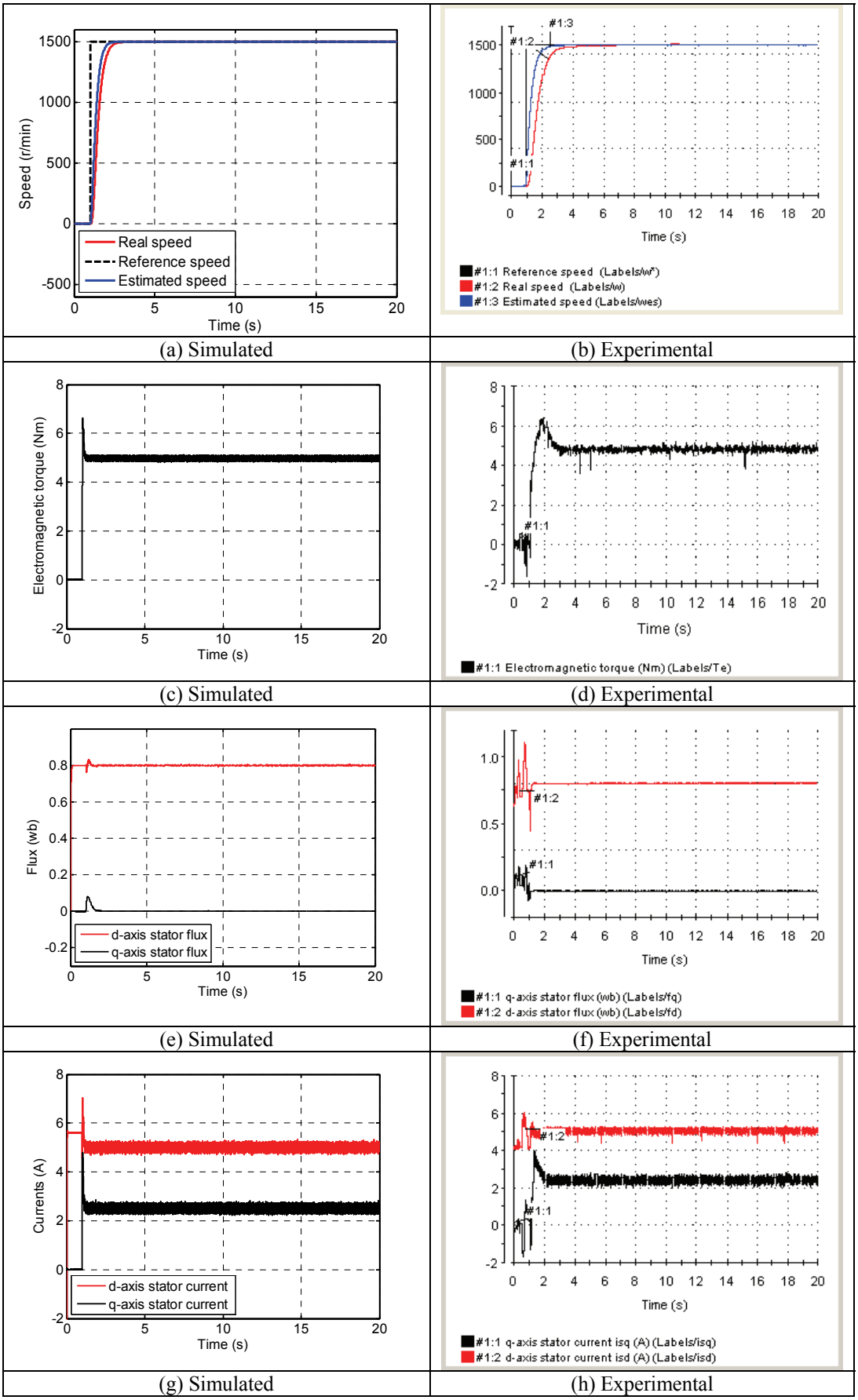
Fig. 4. Scheme used for experimental setup.



(a) Simulated (b) Experimental

Fig. 5. Simulation and experimental results of sensorless ISFOC of the TPIM to a step, the reference speed from 0 to 1500 r/min

In this section, we present simulation and experimental results showing the feasibility of the proposed Sensorless speed control for TPIMD. Here, the reference flux is kept constant at the nominal value 0.8 Wb. For the speed controller an Integral-Proportional (IP) speed controller has been designed in order to stabilize the speed-control loop. The gains of the IP controller are determined using a design method to obtain a damping ratio of 1. Figure 5 shows the simulation and experimental results of the rotor speed based MRAS estimator when the machine is operating from forward zero speed to nominal speed (1500 r/min). It can be seen that at relatively nominal speed, the estimated speed tracks the actual speed reasonably well. As a second test, the starting with the reference of motor speed 1500 r/min and a step in the load torque of 5 Nm at 1s, has been performed (Fig. 6). The difference between the real and observed speeds remains very small even during the very beginning of the transient when the stator flux initialization goes up.



(a) Simulated (b) Experimental

(c) Simulated (d) Experimental

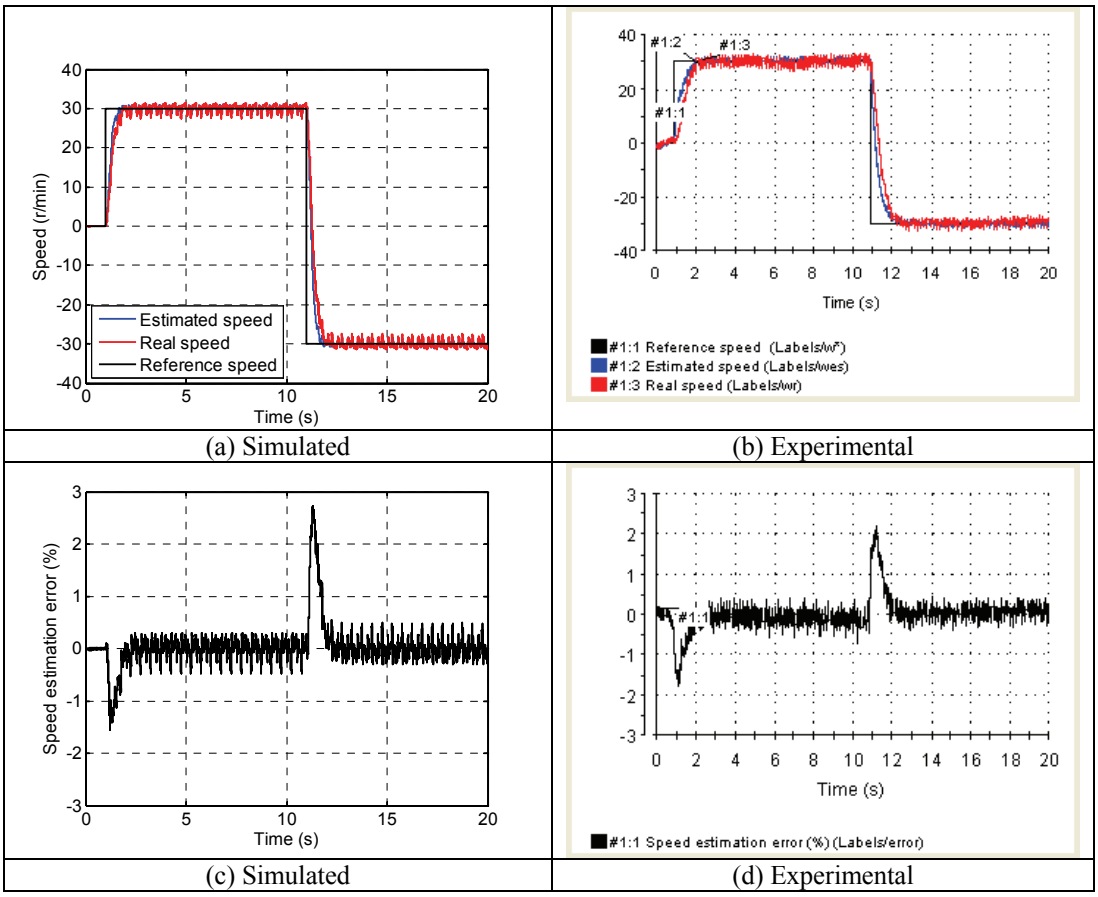
(e) Simulated (f) Experimental

(g) Simulated (h) Experimental

Fig. 6. Simulation and experimental results of sensorless ISFOC of the TPIM in the case when the speed command is 1500 r/min

Figures 6c and d show the estimated electromagnetic torque and in Fig. 6e and f the d, q components of the stator flux are estimated using the measured stator phase currents. The simulation and experimental results presented in Figs. 6e and f show that the stator fluxes converge from their initial values for their final values, respectively ($\phi_{sd} = \phi_{sl}$ and $\phi_{sq} = 0$).

Using the estimated rotor speed as the feedback, the low-speed characteristics of MRAS sensorless control scheme is examined, and the results are shown in Fig. 7. The rotor speed control performance is in the low-speed operation region (30 r/min) of the rotor speed Sensorless drive. It is shown that the proposed algorithm has good speed estimation and adequate vector control characteristics at low rotor speed operation.



(a) Simulated (b) Experimental

(c) Simulated (d) Experimental

Fig. 7. Simulation and experimental results of sensorless ISFOC of the TPIM for reversing speed reference from 30 r/min to -30 r/min

However, it is noticable that the last results show clearly that the proposed MRAS scheme worked successfully for the Two-Phase Induction Motor Sensorless control algorithm.

6. CONCLUSION

This paper makes a contribution to the issue of sensorless ISFOC of TPIMD. Also, it presents experimental results of an efficient sensorless speed field oriented control for TPIMD. The results were satisfactory and the proposed IP controller gives the system good performances and good dynamic behaviour.

The performances of the proposed Model Reference Adaptive System (MRAS) scheme are satisfactory for both high magnitude and small transients. In this way, this technique seems promising to be transferred towards industrial applications where speed sensor is forbidden. The results presented in

this paper show the effectiveness of observation techniques in order to remove speed sensor in vector control drives at nominal, low and zero motor speed reference controls.

NOMENCLATURE

v_{sd}, v_{sq}	d, q-axis stator voltage components
i_{sd}, i_{sq}	d, q-axis stator current components
i_{rd}, i_{rq}	d, q-axis rotor current components
ϕ_{sd}, ϕ_{sq}	d, q-axis stator flux components
ϕ_{rd}, ϕ_{rq}	d, q-axis rotor flux components
R_{sd}, R_{sq}	stator windings resistances
R_r	rotor resistance
L_{sd}, L_{sq}	stator self-inductance
L_r	rotor self-inductances
M_{srd}, M_{srq}	mutual inductances
T_e, T_l	electromagnetic and load torque
p =d/dt	Laplace operator
ω_s , ω	synchronous and rotor angular speed
ω_{sl}	slip angular speed (ω_s -ω)
Ω	mechanical rotor speed
n_p	pole-pair number
f_r	friction coefficient
J	total inertia
σ_d, σ_q	leakage coefficient
τ_{sd}, τ_{sd}, τ_r	stator and Rotor time constant
M. W	main winding
A. W	auxiliary winding
K_{pv}	proportional gain of the IP speed controller
K_{iv}	integral gain of the IP speed controller
K_{ip}	proportional gain of the PI current controller
K_{ii}	integral gain of the PI current controller
*	reference value

REFERENCES

1. Correa, M. R., Jacobina, C. B., Da Silva, E. R. C. & Lima, A. M. N. (2004). Vector control strategies for single-phase induction motor drive systems. *IEEE Trans. Ind. Electron*., Vol. 51, pp. 1073–1080.
2. Ben Azza, H., Jemli, M., Boussak, M. & Gossa, M. (2011). High performance sensorless speed vector control of SPIM drives with on-line stator resistance estimation. *Journ. Simulation Modelling Practice and Theory*, Vol. 19, Issue 1, pp. 271–282.
3. Jemli, M., Ben Azza, H., Boussak, M. & Gossa, M. (2009). Sensorless indirect stator field orientation speed control for single-phase induction motor drive. *IEEE Trans. on Power Electronics*, Vol. 24, No. 6, pp.1618-1627.
4. Correa, M. R., Jacobina, C. B., Lima, A. M. N. & da Silva, E. R. C. (2000). Rotor-flux-oriented control of a single-phase induction motor drive. *IEEE Trans. Ind. Electron*., Vol. 47, No. 4, pp. 832–841.
5. Blaabjerg, F., Lungeanu, F., Skaug, K. & Tonnes, M. (2004). Two-phase induction motor drives low-cost topologies for TPIM drives in industrial applications. *IEEE Trans. Ind. Applic. Mag*., pp. 24–32.
6. Lettenmaier, T. A., Nvotny, D. W. & Lipo, T. A. (1991). Single-phase induction motor with an electronically controlled capacitor. *IEEE Trans. Ind. Appl*., Vol. 27, No. 1, pp. 38–43.
7. Reicy, S. & Vaez-Zadeh, S. (2005). Vector control of single-phase induction machine with maximum torque operation. *Proc. IEEE ISIE*, Dubrovnik, Coroatia.
8. Ben Azza, H., Jemli, M. & Gossa, M. (2008). Full-digital implementation of ISFOC for single-phase induction motor drive using dSpace DS 1104 control board. *International Review of Electrical Engineering (I.R.E.E.)*, Vol. 3, No. 4, pp. 721-729.

9. Correa, M. B. R., Jacobina, C. B., Lima, A. M. N. & da Silva, E. R. C. (2002). Three-leg voltage source inverter for two phase ac motor drive system. *IEEE Trans. on Power Electronics*, Vol. 9, No. 4, pp. 377-383.
10. Jang, D. H. (2007). PWM methods for two-phase induction motors. *IEEE Industry Application Magazine*, Vol.13, No. 2, pp. 50-61.
11. Jang, D. H. & Yoon, D. Y. (2003). Space-vector PWM technique for two-phase inverter-fed two phase induction motors. *IEEE Trans. Ind. Appl*., Vol. 39, No. 2, pp. 542–549.
12. Jabbar, M. A., Khambadkone, A. M. & Yanfeng, Z. (2004). Space-vector modulation in a two-phase induction motor drive for constant-power operation. *IEEE Trans. Ind. Electron*., Vol. 51, No. 5, pp. 1081–1088.
13. Jemli, M., Ben Azza, H. & Gossa, M. (2009). Real-time implementation of IRFOC for single-phase induction motor drive using dSpace DS 1104 control board. *Journ. Simulation Practice and Theory*, Vol. 17, pp. 1071–1080.
14. Kianinezhad, R., Nahid-Mobarakeh, B., Betin, F. & Capolino, G. A. (2009). Robust Sensorless vector control of induction machines. *Iranian Journal of Science & Technology, Transaction B: Engineering*, Vol. 33, No B2, pp. 133–147.
15. Ebrahimi, M., Rezaei, E., Vaseghi, B. & Danesh, M. (2006). Rotor resistance identification using neural networks for induction motor drives in the case of insensitivity to load variations. *Iranian Journal of Science & Technology, Transaction B: Engineering*, Vol. 30, No B2, pp. 223–236.
16. Baabjerg, F., Lungeanu, F., Skaug, K. & Tonnes, M. (2004). Low–cost topologies for TPIM drives. *IEEE Trans. Ind. Applicat. Mag*., pp. 24-32.
17. Vaez-Zadeh, S. & Payman, A. (2003). Design and application of speed estimation for single-phase induction motors. *Proc. EPE 2003, Toulouse, ISBN*: 90-75815-07-7, pp. 1–10.
18. Payman, A. & Vaez-Zadeh, S. (2004). DSP based speed estimation of single phase induction motors. *Proc. 35th Annual IEEE Power Electron. Spec. Conf.*, Aachen, Germany.
19. Vaez-Zadeh, S. & Payman, A. (2006). Design and analysis of sensorless torque optimization for single phase induction motors. *Proc. Int. Journ. Energy Conver. and Manag*., Vol. 47, pp. 1464–1477.
20. Vaez-Zadeh, S. & Reicy, H. S. (2005). Sensorless vector control of single-phase induction motor drives. ICEMS. Proc. *of the Eighth International Conference on Electrical Machines and Systems*, Vol. 3, pp. 1838-1442.
21. Cirrincione, M., Pucci, M., Cirrincione, G. & Capolino, G. A. (2004). A new TLS based MRAS speed estimation with adaptive integration for high performance induction motor drives. *IEEE Transaction on Industry Application*, Vol. 40, No. 4, pp. 1116-1137.
22. Maurizio, C., Marcello, P., Giansalvo, C. & Capolino, G. A. (2005). An MRAS sensorless technique based on the MCA EXIN + Neuron for high performance induction motor drives. *Automatika, ATKAAF*, Vol. 46, pp. 59–72.

APPENDIX

Table A.1: Two-phase induction machine parameters

Specification		Parameters	
Rated power	1.1 kW	R_{sd}	2.473 Ω
Rated voltage	220 V	R_{sq}	6.274Ω
Rated current	6.58 A	R_r	5.514 Ω
Rated frequency	50 hz	L_{sd}	0.0904 H
Number of pole pairs	2	L_{sq}	0.1099 H
Rated speed	1430 r/min	L_r	0.0904 H
		M_{srd}	0.0817 H
		M_{srq}	0.0715 H
		J	$1.2.10^{-3}$ kg.m^2
		f	$0.9.10^{-3}$ N.m.s.rad^{-1}